arXiv:1502.02529v1 [math.NA] 9 Feb 2015

Higher order operator splitting Fourier spectral methods for the Allen–Cahn equation

Jaemin Shin [a], Hyun Geun Lee [a], and June-Yub Lee [b,*]

[a] *Institute of Mathematical Sciences, Ewha Womans University, Seoul 120-750, Korea*

[b] *Department of Mathematics, Ewha Womans University, Seoul 120-750, Korea*

Abstract

The Allen–Cahn equation is solved numerically by operator splitting Fourier spectral methods. The basic idea of the operator splitting method is to decompose the original problem into sub-equations and compose the approximate solution of the original equation using the solutions of the subproblems. Unlike the first and the second order methods, each of the heat and the free-energy evolution operators has at least one backward evaluation in higher order methods. We investigate the effect of negative time steps on a general form of third order schemes and suggest three third order methods for better stability and accuracy. Two fourth order methods are also presented. The traveling wave solution and a spinodal decomposition problem are used to demonstrate numerical properties and the order of convergence of the proposed methods.

Key words: Operator splitting method; Allen–Cahn equation; Heat evolution equation; Free-energy evolution equation; Backward time step; Traveling wave solution; Spinodal decomposition;

1 Introduction

The Allen–Cahn (AC) equation was originally introduced as a phenomenological model for antiphase domain coarsening in a binary alloy [1]:

$$\frac{\partial \phi(\mathbf{x},t)}{\partial t} = -\frac{F'(\phi(\mathbf{x},t))}{\epsilon^2} + \Delta\phi(\mathbf{x},t), \quad \mathbf{x} \in \Omega,\ 0 < t \le T, \tag{1}$$

* Corresponding author
Email address: jyllee@ewha.ac.kr (June-Yub Lee).

where Ω is a domain in $\mathbb{R}^d$ $(d = 1, 2, 3)$. The quantity $\phi(\mathbf{x}, t)$ is defined as the difference between the concentrations of two components in a mixture, for example, $\phi(\mathbf{x}, t) = (m_\alpha - m_\beta)/(m_\alpha + m_\beta)$ where m_α and m_β are the masses of phases α and β. The function $F(\phi) = 0.25(\phi^2 - 1)^2$ is the Helmholtz free-energy density for ϕ, which has a double-well form, and $\epsilon > 0$ is the gradient energy coefficient. The system is completed by taking an initial condition $\phi(\mathbf{x}, 0) = \phi^0(\mathbf{x})$ and a homogeneous Neumann boundary condition $\nabla\phi \cdot \mathbf{n} = 0$, where $\mathbf{n}$ is normal to $\partial\Omega$.

The AC equation and its various modified forms have been applied in addressing a range of problems, such as phase transitions [1], image analysis [2,3], motion by mean curvature [4,5,6], two-phase fluid flows [7], and crystal growth [8,9,10]. Therefore, many researchers have studied numerical methods for solving the AC type equation to improve stability and accuracy and to have a better understanding of its dynamics. Stable time step size of explicit schemes is severely restricted due to the nonlinear term $F'(\phi)$ and implicit schemes suffer from a solvability problem with large time steps. One of considerable semi-implicit methods is unconditionally gradient stable method proposed by Eyre [11], which is first order accurate in time, and unconditionally gradient stable means that a discrete energy non-increases from one time level to the next regardless of the time step size. And the authors in [12,13] proposed first and second order stabilized semi-implicit methods.

Another numerical method employed for solving the AC equation is the operator splitting method [12,14,15]. Operator splitting schemes have been applied for many types of evolution equations [16,17,18,19,20,21]. The basic idea of the operator splitting method is to decompose the original problem into subproblems which are simpler than the original problem and then to compose the approximate solution of the original problem by using the exact or approximate solutions of the subproblems in a given sequential order. Operator splitting methods are simple to implement and computationally efficient to achieve higher order accuracy while semi-implicit schemes are hard to improve the order of convergence. The first and the second order operator splitting methods for the AC equation is quite well-known [12,14,15], however, the higher order (more than two) operator splitting method for the AC equation is less well-known.

In this paper, we investigate higher order operator splitting schemes and propose several higher order methods to solve the AC equation with a Fourier spectral method. We decompose the AC equation into heat and free-energy evolution equations, which have closed-form solutions in the Fourier and physical spaces, respectively. Because the first and second operator splitting methods have only forward time steps, the boundedness of the solution is guaranteed regardless of the time step size [15]. However, we could not guarantee the stability with large time step size since each operator has at least one

backward time step with third and higher order of accuracy [17,18]. Because a backward time marching affects numerical stability on both sub-equations, we consider ways of minimizing the effect of negative time steps and introduce a cut-off function to limit the exponential amplification of high-frequency modes in solving the heat evolution equation.

This paper is organized as follows. In section 2, we briefly review the operator splitting methods which are studied by the authors in [17]. In section 3, we present higher order operator splitting Fourier spectral methods for solving the AC equation. We discuss the stability issues for backward time marching and suggest the three third order operator splitting methods. We present numerical experiments demonstrating numerical properties and the order of convergence of the proposed methods in section 4. Conclusions are drawn in section 5.

2 A brief review on the operator splitting method

In this section, we review some of the basic properties of the operator splitting methods for a time evolution equation with two evolution terms in summarizing the work by D. Goldman and T. Kapper [17]. Let $\mathcal{A}^{a\Delta t}$ be the solution operator for the time evolution equation $\frac{\partial \phi}{\partial t} = f_A(\phi)$, that is $(\mathcal{A}^{a\Delta t}\phi)(t) := \phi(t + a\Delta t)$, and $\mathcal{B}^{b\Delta t}$ be the solution operator for $f_B(\phi)$. Then the operators $\mathcal{A}$ and $\mathcal{B}$ satisfy the semi-group properties. Suppose we want to minimize the number of the operator evaluations of $\mathcal{A}^{a\Delta t}$ and $\mathcal{B}^{b\Delta t}$ in order to get a N-th order approximation of the following ordinary differential equation consists of two evolution terms,

$$\frac{\partial \phi}{\partial t} = f_A(\phi) + f_B(\phi). \tag{2}$$

It is well-known that the simplest form of the first order solution operator for (2) is given as

$$\mathcal{S}^{(1)} = \mathcal{B}^{\Delta t}\, \mathcal{A}^{\Delta t}, \tag{3}$$

that is, $(\mathcal{S}^{(1)}\phi)(t)$ is a first order accurate approximation of $\phi(t+\Delta t)$. Here the choice of $\mathcal{A}$ and $\mathcal{B}$ (or f_A and f_B) is arbitrary, thus without loss of generality, we may assume that the first operator evaluated is always $\mathcal{A}^{a\Delta t}$.

We now consider a solution operator $\mathcal{S}^{(p)}$ with $2p$ (or $2p-1$ if $b_p = 0$) evaluations of the operators $\mathcal{A}$ and $\mathcal{B}$ in the following form,

$$\mathcal{S}^{(p)} = \mathcal{B}^{b_p\Delta t}\, \mathcal{A}^{a_p\Delta t}\, \cdots\, \mathcal{B}^{b_1\Delta t}\, \mathcal{A}^{a_1\Delta t}, \tag{4}$$

where all of $\{a_j\}_{j=1}^{p}$, $\{b_j\}_{j=1}^{p-1}$ are non-zeros. The coefficients $a_1, \ldots, a_p$ and $b_1, \ldots, b_p$ in $\mathcal{S}^{(p)}$ must satisfy certain conditions to make $\mathcal{S}^{(p)}$ an N-th order approximation operator for (2). It is well-known that there exists $\mathcal{S}^{(p)}$ at least N-th order accurate when $p \geq N$. (See [17] and the references therein for

the derivation of the following conditions.) For first-order accuracy, $\{a_j\}$, $\{b_j\}$ must satisfy

$$\sum_{j=1}^{p} a_j = \sum_{j=1}^{p} b_j = 1. \tag{5}$$

For second-order accuracy, $\{a_j\}$ and $\{b_j\}$ must satisfy (5) and the conditions

$$\sum_{j=2}^{p} a_j \left(\sum_{k=1}^{j-1} b_k \right) = \sum_{j=1}^{p} b_j \left(\sum_{k=1}^{j} a_k \right) = \frac{1}{2}. \tag{6}$$

For third-order accuracy, $\{a_j\}$ and $\{b_j\}$ must satisfy (5), (6), and the conditions

$$\sum_{j=2}^{p} a_j \left(\sum_{k=1}^{j-1} b_k \right)^2 = \sum_{j=1}^{p} b_j \left(\sum_{k=1}^{j} a_k \right)^2 = \frac{1}{3}. \tag{7}$$

For a second-order scheme of the form (4) with $p = 2$, $\mathcal{S}^{(2)} = \mathcal{B}^{b_2 \Delta t}\, \mathcal{A}^{a_2 \Delta t}\, \mathcal{B}^{b_1 \Delta t}\, \mathcal{A}^{a_1 \Delta t}$, (5) and (6) give

$$a_1 + a_2 = 1, \quad b_1 + b_2 = 1, \quad a_2 b_1 = \frac{1}{2}. \tag{8}$$

Since there are three equations for the four unknowns, let $b_1{=}\omega$ ($\neq 0$) be a free parameter, then the solution of (8) gives a general form of a second order solution operator with up to 4 operator evaluations,

$$\mathcal{S}_{\omega}^{(2)} = \mathcal{B}^{(1-\omega)\Delta t}\, \mathcal{A}^{\frac{1}{2\omega}\Delta t}\, \mathcal{B}^{\omega \Delta t}\, \mathcal{A}^{(1-\frac{1}{2\omega})\Delta t}. \tag{9}$$

Note that $\mathcal{S}_{\omega}^{(2)} = \mathcal{A}^{\frac{\Delta t}{2}}\, \mathcal{B}^{\Delta t}\, \mathcal{A}^{\frac{\Delta t}{2}}$ with $\omega = 1$ is the simplest form (with only three evaluations) among second order operators since two evaluations of $\mathcal{A}$ and $\mathcal{B}$ is not enough to make it second order accurate.

For a third-order scheme of the form

$$\mathcal{S}^{(3)} = \mathcal{B}^{b_3 \Delta t}\, \mathcal{A}^{a_3 \Delta t}\, \mathcal{B}^{b_2 \Delta t}\, \mathcal{A}^{a_2 \Delta t}\, \mathcal{B}^{b_1 \Delta t}\, \mathcal{A}^{a_1 \Delta t}, \tag{10}$$

(5), (6), and (7) give

$$a_1 + a_2 + a_3 = 1, \quad b_1 + b_2 + b_3 = 1, \quad a_2 b_1 + a_3(b_1 + b_2) = \frac{1}{2}, \tag{11}$$

$$a_2 b_1^2 + a_3(b_1 + b_2)^2 = \frac{1}{3}, \quad b_1 a_1^2 + b_2(a_1 + a_2)^2 + b_3 = \frac{1}{3}. \tag{12}$$

Choosing $b_3 = \omega$ to be a free parameter, we can obtain two branches of the solution for (11) and (12),

$$b_1^{\pm} = \frac{1-\omega}{2} \mp \frac{\sqrt{D(\omega)}}{2(4\omega - 1)}, \quad a_2 = \frac{4\omega - 1}{2(3\omega - 1)}, \quad a_3^{\pm} = \frac{\frac{1}{2} - b_1^{\pm} a_2}{1 - \omega},$$

$$a_1^{\pm} = 1 - a_2 - a_3^{\pm}, \quad b_2^{\pm} = 1 - b_1^{\pm} - b_3,$$

where

$$D(\omega) = (\omega - 1)^2(4\omega - 1)^2 + 12(4\omega - 1)\left(\omega - \frac{1}{3}\right)^2.$$

Note that real solutions of (11) and (12) are only possible for $\omega > \frac{1}{4}$ and $\omega \le \omega^*$, where $\omega^* \approx -1.217\cdots$ is the real root of $D(\omega)/(4\omega - 1) = 0$.

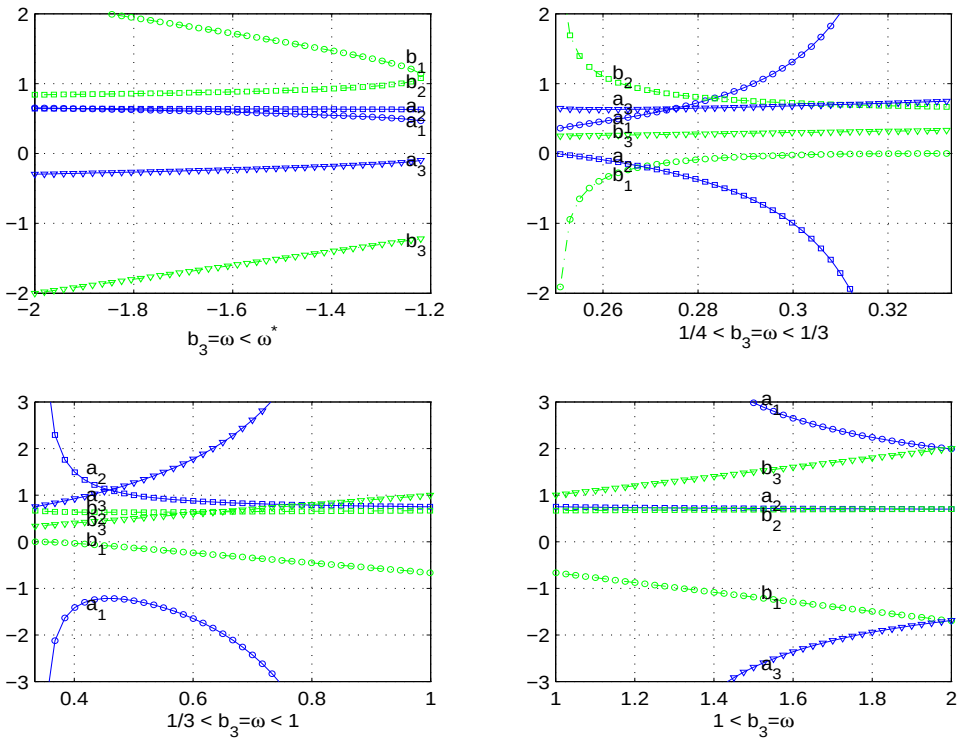

Fig. 1. Positive branch solutions, $a_1^+, b_1^+, a_2^+, b_2^+, a_3^+, b_3^+$ as a function of $b_3^+ = \omega$

Figure 1 shows the positive branch solutions, $a_1^+, b_1^+, a_2^+, b_2^+, a_3^+, b_3^+$ as a function of $b_3^+ = \omega$ for the third order operator $\mathcal{S}^{(3)}_{\omega^+}$ and Figure 2 shows the negative branch solutions for $\mathcal{S}^{(3)}_{\omega^-}$. In any case, there exists exactly one negative value among a_1, a_2, a_3 and also only one negative value among b_1, b_2, b_3. There are three special cases when the solutions may blow up. As $\omega \to \frac{1}{4}^+$, $\mathcal{S}^{(3)}_{\omega^\pm}$ with $a_2 = 0$, $b_2^{\pm} + b_1^{\pm} = \frac{3}{4}$ degenerates into a second order operator, $\mathcal{B}^{\frac{1}{4}\Delta t}\,\mathcal{A}^{\frac{2}{3}\Delta t}\,\mathcal{B}^{\frac{3}{4}\Delta t}\,\mathcal{A}^{\frac{1}{3}\Delta t}$. As $\omega \to \frac{1}{3}$, $\mathcal{S}^{(3)}_{\omega^\pm}$ with $b_1^+ = 0$, $a_1^+ + a_2^+ = \frac{1}{4}$ or $b_2^- = 0$, $a_2^- + a_3^- = \frac{3}{4}$ degenerates into a second order operator, $\mathcal{B}^{\frac{1}{3}\Delta t}\,\mathcal{A}^{\frac{3}{4}\Delta t}\,\mathcal{B}^{\frac{2}{3}\Delta t}\,\mathcal{A}^{\frac{1}{4}\Delta t}$. As $\omega \to 1$, the negative branch solutions have removable singularities and $\mathcal{S}^{(3)}_{\omega^-}$ converges to $\mathcal{B}^{\Delta t}\,\mathcal{A}^{\frac{-1}{24}\Delta t}\,\mathcal{B}^{\frac{-2}{3}\Delta t}\,\mathcal{A}^{\frac{3}{4}\Delta t}\,\mathcal{B}^{\frac{2}{3}\Delta t}\,\mathcal{A}^{\frac{7}{24}\Delta t}$ whereas the positive branch solution does not provide a convergent operator.

We remark that a symmetric $\mathcal{S}^{(3)}$ with $b_3 = 0$, $a_1 = a_3$, and $b_1 = b_2$ satisfying (5), (6) has only a second-order accuracy, that is, $a_1 = \frac{1}{6}$, $b_1 = \frac{1}{2}$, and $a_2 = \frac{2}{3}$ does not satisfy (7). However, a symmetric $\mathcal{S}^{(4)}$ with $b_4 = 0$, $a_1 = a_4$, $a_2 = a_3$,

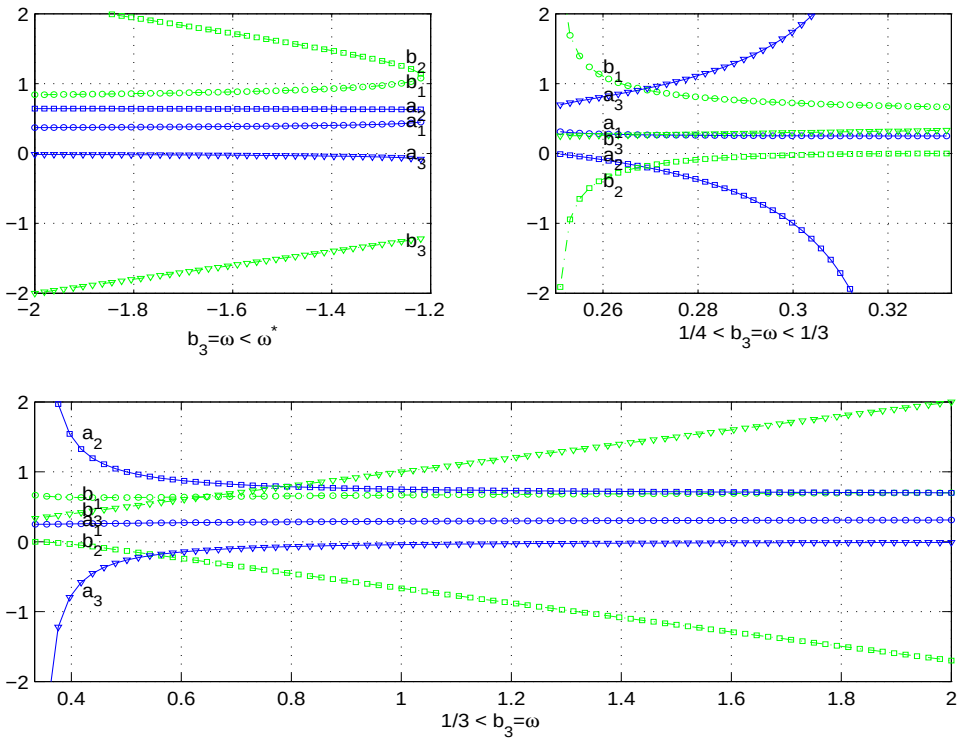

Fig. 2. Negative branch solutions, $a_1^-, b_1^-, a_2^-, b_2^-, a_3^-, b_3^-$ as a function of $b_3^- = \omega$ and $b_1 = b_3$ satisfying only (5), (6), and (7),

$$\mathcal{S}_U^{(4)} := \mathcal{A}^{\frac{\omega}{2}\Delta t}\, \mathcal{B}^{\omega\Delta t}\, \mathcal{A}^{\frac{1-\omega}{2}\Delta t}\, \mathcal{B}^{(1-2\omega)\Delta t}\, \mathcal{A}^{\frac{1-\omega}{2}\Delta t}\, \mathcal{B}^{\omega\Delta t}\, \mathcal{A}^{\frac{\omega}{2}\Delta t} \tag{13}$$

happens to be a fourth-order accuracy with $\omega = \omega_U = 1/(2-2^{1/3}) \approx 1.3512$, $\frac{1-\omega}{2} \approx -0.1756$, and $1-2\omega \approx -1.7024$. This is the simplest form of fourth order operator with only 7 operator evaluations and this can be derived as a symmetric combination of a second order operator $\mathcal{T}^{\Delta t} := \mathcal{A}^{\frac{\Delta t}{2}}\, \mathcal{B}^{\Delta t}\, \mathcal{A}^{\frac{\Delta t}{2}}$,

$$\mathcal{S}_U^{(4)} := \mathcal{T}^{\omega\Delta t}\, \mathcal{T}^{(1-2\omega)\Delta t}\, \mathcal{T}^{\omega\Delta t}, \quad \omega = \omega_U.$$

Another a well-known fourth order operator splitting method [22] can be also derived as a symmetric combination of the second order operator $\mathcal{T}^{\Delta t}$,

$$\begin{aligned}\mathcal{S}_V^{(6)} &:= \mathcal{T}^{\omega\Delta t}\, \mathcal{T}^{\omega\Delta t}\, \mathcal{T}^{(1-4\omega)\Delta t}\, \mathcal{T}^{\omega\Delta t}\, \mathcal{T}^{\omega\Delta t} \\ &= \mathcal{A}^{\frac{\omega}{2}\Delta t}\mathcal{B}^{\omega\Delta t}\mathcal{A}^{\omega\Delta t}\mathcal{B}^{\omega\Delta t}\mathcal{A}^{\frac{1-3\omega}{2}\Delta t}\mathcal{B}^{(1-4\omega)\Delta t}\mathcal{A}^{\frac{1-3\omega}{2}\Delta t}\mathcal{B}^{\omega\Delta t}\mathcal{A}^{\omega\Delta t}\mathcal{B}^{\omega\Delta t}\mathcal{A}^{\frac{\omega}{2}\Delta t}\end{aligned} \tag{14}$$

with $\omega = \omega_V = 1/(4-4^{1/3}) \approx 0.4145$. The $\mathcal{S}_V^{(6)}$ method is computationally less efficient (11 operator evaluations compared to minimum of 7 evaluations) but has better stability condition ($\frac{1-3\omega}{2} \approx -0.1217$, $1-4\omega \approx -0.6580$) than the method defined in (13).

We close this section with a remark that not just the third and the fourth

order methods mentioned above but any operator splitting methods of third or higher order contains at least one negative time steps for each of the operators, $\mathcal{A}$, $\mathcal{B}$. (See [17,18] for the proof of the general theorem.)

3 Higher-order operator splitting Fourier spectral methods

We consider the AC equation (1) in one-dimensional space $\Omega = (0, L)$. Two- and three-dimensional spaces can be analogously defined. For simplicity of notation, we sometimes abuse the notation $\phi = \phi(t)$ referring $\phi(\cdot, t)$ and define the "*free-energy evolution operator*" $\mathcal{F}^{\Delta t}$ as follows

$$\mathcal{F}^{\Delta t}(\phi(t^n)) := \phi(t^n + \Delta t), \tag{15}$$

where $\phi(t^n + \Delta t)$ is a solution of the first order differential equation

$$\frac{\partial \phi}{\partial t} = -\frac{F'(\phi)}{\epsilon^2}$$

with an initial condition $\phi(t^n)$. For given $F'(\phi) = \phi^3 - \phi$, we have an analytical formula (See [12,14,15]) for the evolution operator $\mathcal{F}^{\Delta t}$ in the physical space

$$\mathcal{F}^{\Delta t}(\phi) = \frac{\phi}{\sqrt{\phi^2 + (1-\phi^2)e^{-\frac{2\Delta t}{\epsilon^2}}}}. \tag{16}$$

We also define the "*heat evolution operator*" $\mathcal{H}^{\Delta t}$ as follows

$$\mathcal{H}^{\Delta t}(\phi(t^n)) := \phi(t^n + \Delta t), \tag{17}$$

where $\phi(t^n + \Delta t)$ is a solution of the first order differential equation

$$\frac{\partial \phi}{\partial t} = \Delta \phi$$

with an initial condition $\phi(t^n)$. In this paper, we employ the discrete cosine transform [23] to solve the AC equation with the zero Neumann boundary condition: for $k = 0, \ldots, M-1$,

$$\widehat{\phi}_k = \alpha_k \sum_{l=0}^{M-1} \phi_l \cos\left[\frac{\pi}{M} k \left(l + \frac{1}{2}\right)\right],$$

where $\phi_l = \phi\left(\frac{L}{M}\left(l+\frac{1}{2}\right)\right)$ and $\alpha_0 = \sqrt{1/M}$, $\alpha_k = \sqrt{2/M}$ for $k \geq 1$. Then, we have a semi-analytical formula for the evolution operator $\mathcal{H}^{\Delta t}$ in the discrete cosine space

$$\mathcal{H}^{\Delta t}(\phi) = \mathcal{C}^{-1}\left[\, e^{A_k \Delta t} \mathcal{C}\left[\phi\right]\right], \tag{18}$$

where $A_k = -\left(\frac{\pi k}{L}\right)^2$ and $\mathcal{C}$ denotes the discrete cosine transform.

For the first order operator splitting scheme $\mathcal{S}^{(1)}$ in (3) and the second order scheme $\mathcal{S}^{(2)}_\omega$ in (9) with $0 < \omega \leq 1$, the evaluations are all forward time marching, that is, all of $\{a_j\}_{j=1}^p$ and $\{b_j\}_{j=1}^p$ are positive. We can easily show that both schemes are unconditionally stable, in the sense that $|\phi(t^n+\Delta t)| \leq 1$ if $|\phi(t^n)| \leq 1$ regardless of the time step size. (See [15] for the proof.) However, in the case of third or higher order, each of operators $\mathcal{F}$, $\mathcal{H}$ has at least one backward evaluation as mentioned in section 2. For this reason, we need to investigate the stability of the operators $\mathcal{F}^{-\Delta t}$ and $\mathcal{H}^{-\Delta t}$ especially for large Δt.

The stability issue for backward time heat equation is well-known. Even though $\mathcal{H}^{\pm\Delta t}\ \mathcal{H}^{\mp\Delta t}$ (without noise) is always an identity operator regardless of the size of Δt, the numerical composition of the operators (even with small error) is far away from the identity operator when Δt becomes large since $\mathcal{H}^{-\Delta t}$ is exponentially big for $\Delta t \gg 1$. The stability of the numerical composition of the free energy evolution operators is less well-known and we want to explain why the numerical composition of the operators $\mathcal{F}^{\pm\Delta t}\ \mathcal{F}^{\mp\Delta t}$ (even with small error) is far away from the identity operator when Δt becomes large using the following figure.

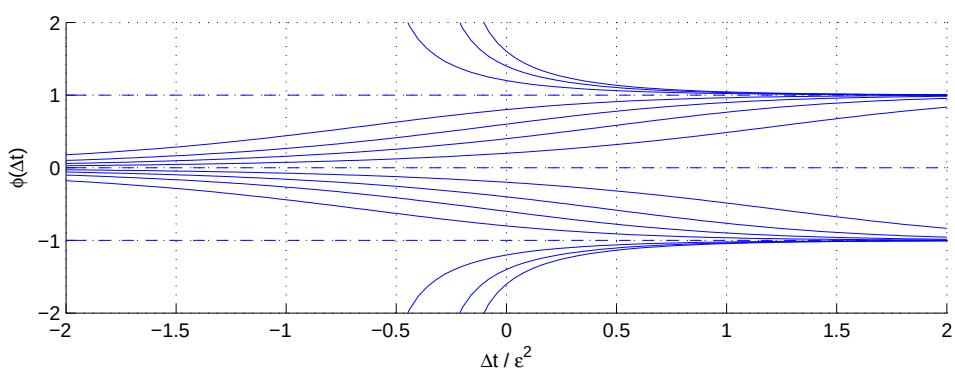

Fig. 3. $\phi(\Delta t) = \mathcal{F}^{\Delta t}(\phi(0))$ with various initial values, $\phi(0) = -1.6, -1.4, \cdots, 1.6$

Figure 3 plots $\mathcal{F}^{\Delta t}(\phi)$ as a function of Δt with various initial values of ϕ between -1.6 to 1.6. As you can see, $\mathcal{F}^{\Delta t}(\phi)$ with $|\phi| < 1$ converges to ± 1 as $\Delta t \gg 1$, however, the solution with $|\phi| > 1$ as a result of small perturbation may blow up when $\Delta t \ll -1$. Therefore, composition of two operators $\mathcal{F}^{\Delta t}$ followed by $\mathcal{F}^{-\Delta t}$ even with small evaluation error near 1 is no longer bounded as Δt is getting bigger. And $\mathcal{F}^{-\Delta t}(\phi)$ with $|\phi| < 1$ converges to 0 for $\Delta t \gg 1$ thus $\mathcal{F}^{-\Delta t}$ followed by $\mathcal{F}^{\Delta t}$ for $\Delta t \gg 1$ may change the sign of result even with small perturbation near 0. This non-linear stability effect is basically a consequence of the fact that the solution of the free-energy evolution operator $\mathcal{F}^{\Delta t}(\phi)$ is exponentially close to 1 or 0 as $\Delta t \to \pm\infty$.

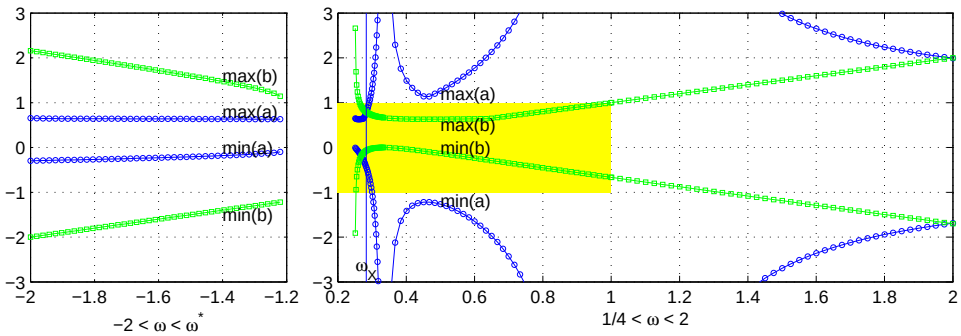

Fig. 4. Minimum and maximum of $\{a_i^+\}_{i=1}^3$ and $\{b_j^+\}_{j=1}^3$ as a function of $b_3^+ = \omega$. The region where values are bounded by $[-1, 1]$ is shaded in yellow.

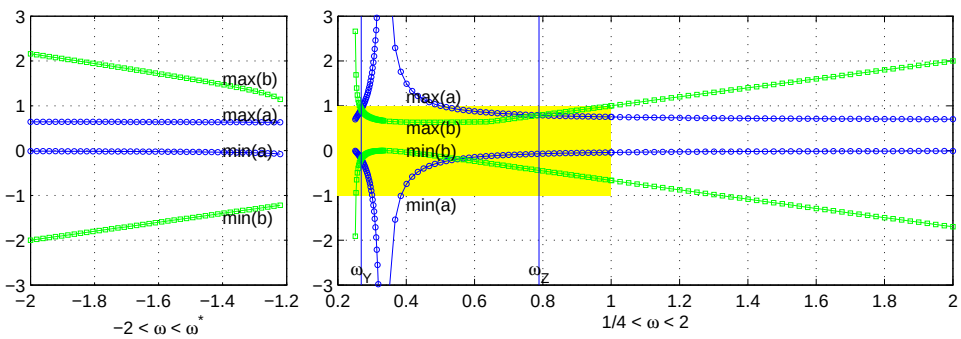

Fig. 5. Minimum and maximum of $\{a_i^-\}_{i=1}^3$ and $\{b_j^-\}_{j=1}^3$ as a function of $b_3^- = \omega$. The region where values are bounded by $[-1, 1]$ is shaded in yellow.

In order to achieve a better stability condition, we propose third order schemes with bounded values of $\{a_j, b_j\}_{j=1}^p$. Figures 4 and 5 show the minimum and maximum values of $\{a_j\}_{j=1}^3$ and $\{b_j\}_{j=1}^3$ for the positive and negative branches, respectively. It is worth noting that $a_1^+, b_1^+, a_2^+, b_2^+, a_3^+, b_3^+$ are bounded by $[-1, 1]$ when $0.26376\cdots \leq \omega^+ \leq 0.29167\cdots$ and $a_1^-, b_1^-, a_2^-, b_2^-, a_3^-, b_3^-$ are bounded by $[-1, 1]$ when $0.26376\cdots \leq \omega^- \leq 0.27362\cdots$ or $1/2 \leq \omega^- \leq 1$. Since there is exactly one negative value among $\{a_j\}_{j=1}^3$, $\max\{a_j\}_{j=1}^3 \geq -\min\{a_j\}_{j=1}^3$ can be inferred from (5) when $|a_j| \leq 1$. Similarly $\max\{b_j\}_{j=1}^3 \geq -\min\{b_j\}_{j=1}^3$ when $|b_j| \leq 1$. In the shaded regions on the figures where values of $|a_j|, |b_j|$ are bounded by 1, there are three local minima of $\max\{|a_j|, |b_j|\}_{j=1}^3$ at which values are summarized on the following table.

Table 1
Solutions for $\mathcal{S}_{\omega^\pm}^{(3)}$, $a_1^\pm, b_1^\pm, a_2^\pm, b_2^\pm, a_3^\pm, b_3^\pm$ at the local minima of $\max\{|a_j|, |b_j|\}_{j=1}^3$.

$\omega^\pm$	Condition	a_1	b_1	a_2	b_2	a_3	b_3
ω_X	$a_1^+ = b_2^+$	0.78868..	-0.07189..	-0.44191..	0.78868..	0.65324..	0.28322..
ω_Y	$b_1^- = a_3^-$	0.26833..	0.91966..	-0.18799..	-0.18799..	0.91966..	0.26833..
ω_Z	$a_2^- = b_3^-$	0.28322..	0.65324..	0.78868..	-0.44191..	-0.07189..	0.78868..

It is worth to note that the sets of $\{a_j^-\}_{j=1}^3$ and $\{b_j^-\}_{j=1}^3$ are same for $\omega^- = \omega_Y$. The set $\{a_j^+\}_{j=1}^3$ for $\omega^+ = \omega_X$ is $\{b_j^-\}_{j=1}^3$ for $\omega^- = \omega_Z$ and the set $\{b_j^+\}_{j=1}^3$ for

$\omega^+ = \omega_X$ is $\{a_j^-\}_{j=1}^3$ for $\omega^- = \omega_Z$. This symmetry gives us a freedom to choose the order of operator evaluations and we define three third order operator splitting methods $\mathcal{S}_X^{(3)}, \mathcal{S}_Y^{(3)}, \mathcal{S}_Z^{(3)}$ for the AC equation as follows:

$$\mathcal{S}_X^{(3)}, \mathcal{S}_Y^{(3)}, \mathcal{S}_Z^{(3)} := \mathcal{F}^{b_3\Delta t}\, \mathcal{H}^{a_3\Delta t}\, \mathcal{F}^{b_2\Delta t}\, \mathcal{H}^{a_2\Delta t}\, \mathcal{F}^{b_1\Delta t}\, \mathcal{H}^{a_1\Delta t} \tag{19}$$

where $\{a_j\}_{j=1}^3$ and $\{b_j\}_{j=1}^3$ are given in Table 1.

Another issue raised with negative time step is that the heat evolution operator $\mathcal{H}^{a_j\Delta t}, a_j < 0$ may amplify the high frequency modes exponentially big, $e^{A_k a_j \Delta t} \gg 1$. This situation $-A_k\Delta t = \left(\frac{\pi k}{L}\right)^2 \Delta t \gg 1$ happens when $k^2\Delta t \gg O(1)$. On the other hand, a physically reasonable bound for Δt in the AC equation is $\frac{\Delta t}{\epsilon^2} \leq O(1)$, thus the blow-up may occur only for physically too high frequency modes, $k \gg \frac{L}{\epsilon}$. Thus, we introduce a cut-off function to bound of $\mathcal{H}^{a_j\Delta t}$ for high frequency modes where $-A_k\Delta t \gg 1$. We will numerically demonstrate the effect of introducing the cut-off function in subsection 4.1.

4 Numerical experiments

In this section, we numerically demonstrate the order of convergence of the proposed third order schemes $\mathcal{S}_X^{(3)}, \mathcal{S}_Y^{(3)}, \mathcal{S}_Z^{(3)}$ in (19) and the fourth order schemes $\mathcal{S}_U^{(4)}$ in (13) and $\mathcal{S}_V^{(6)}$ in (14). Two examples are used for the test, one is the traveling wave solution with analytic solution and the other is a three-dimensional spinodal decomposition problem with random initial values.

One of the well-known traveling wave solutions of the Allen–Cahn equation is

$$\phi(x,t) = \frac{1}{2}\left(1 - \tanh\frac{x - 0.5 - st}{2\sqrt{2}\epsilon}\right), \tag{20}$$

where $s = 3/(\sqrt{2}\epsilon)$ is the speed of the traveling wave. The leftmost plot in Figure 6 shows the initial profile $\phi(x,0)$ and the analytic solution $\phi(x,T_f)$ at $T_f = 1/s$ with $\epsilon = 0.03\sqrt{2}$. Using this traveling wave solution, we compare the first, second, third, and fourth order operator splitting Fourier spectral methods described in section 3. The numerical solutions $\phi(x,t),\ 0 < t \leq T_f$ are obtained with various time step sizes Δt but the spatial grid size is fixed to $h = 2^{-5}$ which provides enough spatial accuracy. The traveling wave solution with the same numerical parameters are used in the following two subsections to test the third and the fourth order schemes.

The rightmost plot in Figure 6 shows the numerical error of the first order scheme $\mathcal{S}^{(1)}$ in (3) and the second order scheme $\mathcal{S}_{\omega=1}^{(2)}$ in (9) compared to the

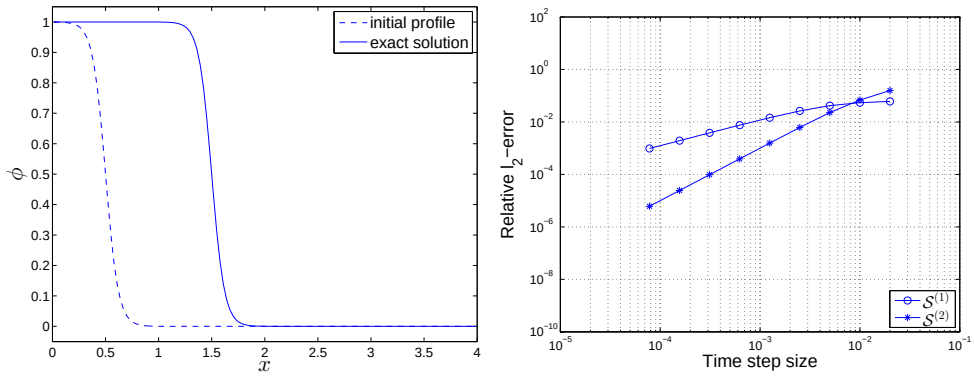

Fig. 6. Traveling wave solution $\phi(x, T_f)$ at $T_f = 1/s$ with $\epsilon = 0.03\sqrt{2}$. And relative l_2 errors of $\phi(x, T_f)$ by $\mathcal{S}^{(1)}, \mathcal{S}^{(2)}$ with $h = 2^{-5}$ for various time step sizes Δt.

analytic solution at $t = T_f$. It is worth to remind that the first and the second order schemes apply only forward time steps of $\mathcal{F}$ and $\mathcal{H}$, thus the stability (or boundedness of the solution) regardless of the size Δt can be easily proven. (See our previous paper [15] for numerical properties of these first and second order schemes.)

4.1 Cut-off function and stability of the third order methods

As mentioned in section 3, negative time steps of $\mathcal{F}$ and $\mathcal{H}$ are unavoidable in the third or higher order operator splitting methods. Especially a negative time step makes the heat evolution operator exponentially big, therefore, we introduce the following cut-off function with a tolerance K_{tol} for the heat evolution operator $\mathcal{H}$,

$$\mathcal{H}^{a_j \Delta t}(\phi) = \mathcal{C}^{-1}\left[\min\{e^{A_k a_j \Delta t}, K_{tol}\} \;\; \mathcal{C}\left[\phi\right]\right]. \tag{21}$$

The choice of K_{tol} depends on the time step size $a_j \Delta t$ and highest frequency modes k_{max} which are functions of desired computational accuracy. Following computational examples in this subsection give a basic guideline for the choice of K_{tol}.

As mentioned in section 2, we have various coefficients $\{a_j^{\pm}\}_{j=1}^{3}$ and $\{b_j^{\pm}\}_{j=1}^{2}$ as a function of $b_3^{\pm} = \omega$. To investigate the effect of ω in the third order method $\mathcal{S}_{\omega}^{(3)}$, we consider the traveling wave problem given in (20). We compute relative l_2 errors for various ω values with a fixed time step $\Delta t = 2^{-4}/s$ and Figures 7 (a) and (b) show relative l_2 errors of the traveling wave solution $\phi(x, T_f)$ by the third order methods $\mathcal{S}_{\omega}^{(3)}$ for positive and negative branches of various ω, respectively. Here we set $K_{tol} = 10^4$ (blue solid line) or 10^9 (green dashed line).

The first noticeable point in Figure 7 might be that the error is relatively large at $\omega^{\pm} \to \frac{1}{4}^{+}$ or $\omega^{\pm} \to \frac{1}{3}$ where the third order operator degenerates into

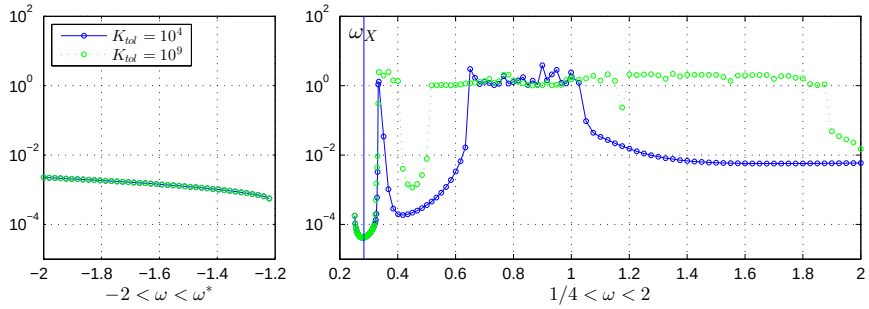

(a) With positive branch solutions for $\mathcal{S}_\omega^{(3)}$ in (10)

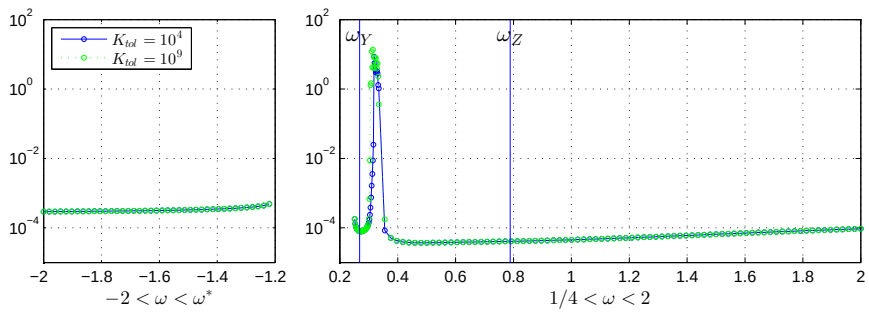

(b) With negative branch solutions for $\mathcal{S}_\omega^{(3)}$ in (10)

Fig. 7. Relative l_2 errors of the traveling wave solution $\phi(x, T_f = 1/s)$ by the third order method $\mathcal{S}_\omega^{(3)}$ for various ω with $\Delta t = 2^{-4}/s$, $\epsilon = 0.03\sqrt{2}$, and $h = 2^{-5}$.

a second order operator. Also a region near $\omega^+ = 1$ in the positive branch case, the computation does not provide any accuracy at all. As $\omega^+ \to 1$, $\mathcal{S}_\omega^{(3)}$ contains a big negative time step of the heat evolution operator $\mathcal{H}^{a_j \Delta t}$ since $\min\{a_j\} \to -\infty$. In these cases, the choice of cut-off parameter K_{tol} becomes important, and small K_{tol} is recommended when $-\min\{a_j\}\Delta t \gg \left(\frac{L}{\pi k_{max}}\right)^2$.

For $0.26376\cdots \leq \omega^+ \leq 0.29167\cdots$ in which $\{a_j^+\}$ and $\{b_j^+\}$ are bounded by $[-1, 1]$, especially near ω_X at which $\max\{|a_j|, |b_j|\}$ has a local minimum, the error is smaller than that for other ω values. The similar phenomenon is observed the computation for the negative branch. We choose three special values $\omega^+ = \omega_X$, $\omega^- = \omega_Y$, and $\omega^- = \omega_Z$ for $\mathcal{S}_X^{(3)}$, $\mathcal{S}_Y^{(3)}$, and $\mathcal{S}_Z^{(3)}$, respectively. For these cases, all $\{a_j\}$ are bounded by $[-1, 1]$ and the choice of cut-off value K_{tol} does not play an important role in the computation.

We now investigate the effect of highest frequency k_{max} to K_{tol}. Plots in Figure 8 show relative l_2 errors of the traveling wave solution $\phi(x, T_f)$ by the third order method $\mathcal{S}_Y^{(3)}$ with different spatial grid sizes $h = \frac{L}{M} = \frac{4}{256} = 2^{-6}$ or $h = \frac{4}{1024} = 2^{-8}$. If a cut-off function is not used (labeled as $K_{tol} = \text{Inf}$), the computation provides no accuracy for relatively large time step. The computation may even stop as two biggest Δt cases for $M = 1024$ and the cases happen more often as $k_{max} = M$ becomes large. If Δt is larger than ϵ^2, K_{tol} must be properly chosen in order to valence the accuracy loss while avoiding

blow-up. However, the choice of K_{tol} makes no significant difference of the solution when $\Delta t \leq \epsilon^2$ (which is physically valid limit for the AC equation) since the high frequency modes $\widehat{\phi}_k$ with $k \gg \frac{L}{\epsilon}$ is negligible for the physically meaningful solution of the AC equation. So the simplest rule of thumb might be setting K_{tol} around the desired accuracy of the computation.

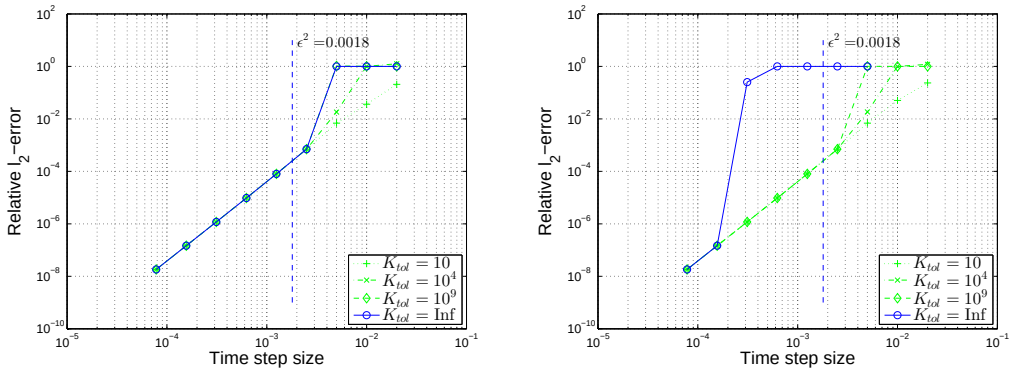

(a) $M = 256$ (b) $M = 1024$

Fig. 8. Relative l_2 errors of the traveling wave solution $\phi(x, T_f = 1/s)$ by $\mathcal{S}_Y$ with $\epsilon = 0.03\sqrt{2}$.

4.2 Convergence of the third and the fourth order methods

We implement the proposed third order schemes $\mathcal{S}_X^{(3)}, \mathcal{S}_Y^{(3)}, \mathcal{S}_Z^{(3)}$ in (19) and the fourth order schemes $\mathcal{S}_U^{(4)}$ in (13) and $\mathcal{S}_V^{(6)}$ in (14). We set the spectral grid size $h = 2^{-5}$, the cut-off limit $K_{tol} = 10^9$ and compare the numerical solutions for various time step sizes Δt with the analytic solution (20) with $\epsilon = 0.03\sqrt{2}$. Figure 9 numerically indicates that the proposed methods have the third and the fourth order accuracy, respectively.

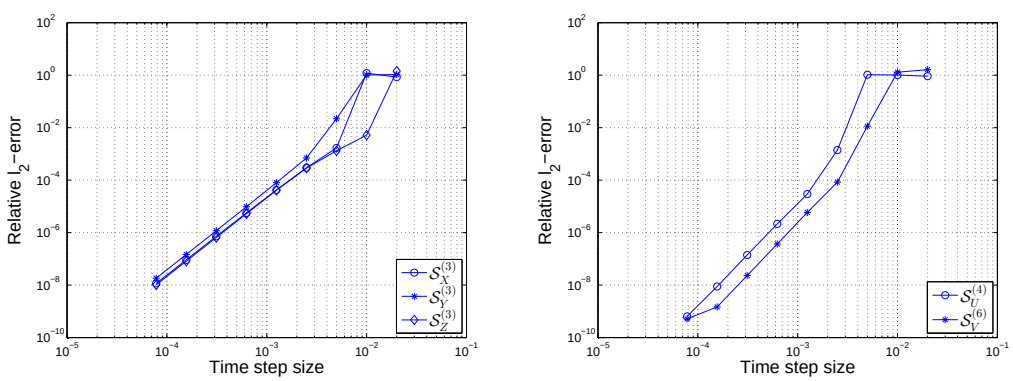

(a) (b)

Fig. 9. Relative l_2 errors of the traveling wave solution $\phi(x, T_f)$ at $T_f = 1/s$ by (a) the third order methods $\mathcal{S}_X^{(3)}$, $\mathcal{S}_Y^{(3)}$, $\mathcal{S}_Z^{(3)}$ (b) the fourth order schemes $\mathcal{S}_U^{(4)}$, $\mathcal{S}_V^{(6)}$

4.3 Convergence of the spinodal decomposition problem in 3D

In this subsection, we compute a spinodal decomposition problem satisfying the AC equation (1) in three-dimensional space with $\epsilon = 0.015$. The intervals $(-1, -1/\sqrt{3})$ and $(1/\sqrt{3}, 1)$ where $F''(\phi) > 0$ are called metastable intervals and $(-1/\sqrt{3}, 1/\sqrt{3})$ where $F''(\phi) < 0$ is called the spinodal interval [24]. It is known that ϕ which lies in the spinodal interval is very unstable and the growth of instabilities results in phase separation, which is called spinodal decomposition. In order to check the numerical convergence, we integrate $\phi(x, y, z, t)$ up to time $T_f = 0.01$ by the proposed numerical schemes with various time step sizes $\Delta t = 10^{-3}/2, \cdots, 10^{-3}/2^7$. The initial condition is given on the computational grid with $h = 2^{-6}$ in the domain $\Omega = [0, 1] \times [0, 1] \times [0, 1]$ as $\phi(x, y, z, 0) = 0.005 \cdot \text{rand}(x, y, z)$ where $\text{rand}(x, y, z)$ is a random number between -1 and 1. Figure 10 shows the initial and the reference solutions at $t = 10^{-3}, 10^{-2}$ computed by the fourth order numerical scheme $\mathcal{S}_V^{(6)}$ with the numerical parameters $K_{tol} = 10^9$ and $\Delta t = 10^{-3}/2^8$.

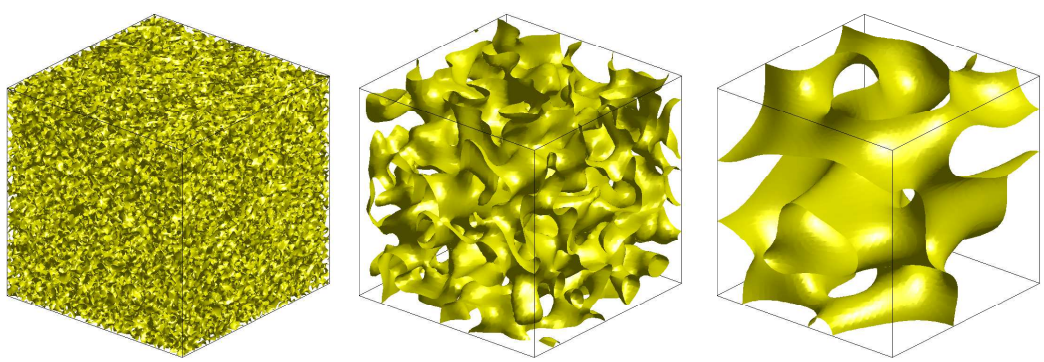

$t = 0$ $\quad$ $t = 10^{-3}$ $\quad$ $t = 10^{-2}$

Fig. 10. The reference solutions $\phi(x, y, z, t)$ by the fourth order method $\mathcal{S}_V^{(6)}$ with $K_{tol} = 10^9$, and $\Delta t = 10^{-3}/2^8$.

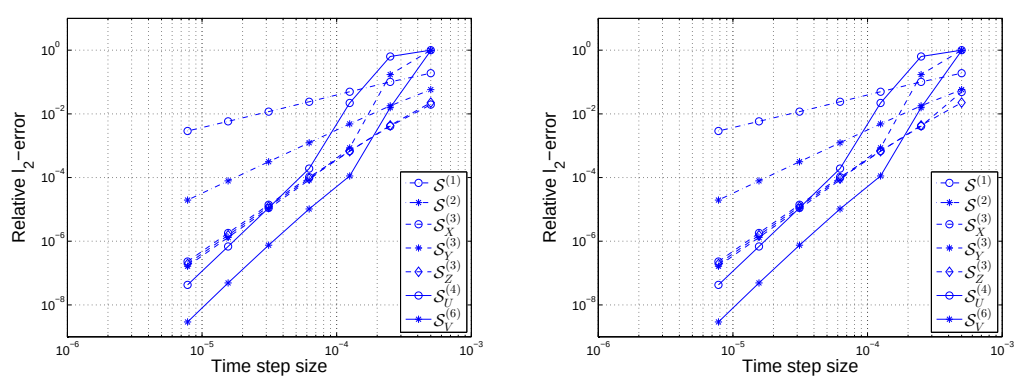

(a) $K_{tol} = 10^4$ $\quad$ (b) $K_{tol} = 10^9$

Fig. 11. Relative l_2 errors of $\phi(x, y, z, T_f = 0.01)$ by $\mathcal{S}^{(1)}$, $\mathcal{S}_{\omega=1}^{(2)}$, $\mathcal{S}_X^{(3)}$, $\mathcal{S}_Y^{(3)}$, $\mathcal{S}_Z^{(3)}$, $\mathcal{S}_U^{(4)}$, $\mathcal{S}_V^{(6)}$ with various time step sizes $\Delta t = 10^{-3}/2, \cdots, 10^{-3}/2^7$.

We also implement the first order scheme $\mathcal{S}^{(1)}$ in (3), the second order scheme $\mathcal{S}^{(2)}_{\omega=1}$ in (9), the proposed third order schemes $\mathcal{S}^{(3)}_X, \mathcal{S}^{(3)}_Y, \mathcal{S}^{(3)}_Z$ in (19), and the fourth order schemes $\mathcal{S}^{(4)}_U$ in (13) and $\mathcal{S}^{(6)}_V$ in (14). The numerical results in Figure 11 show that the cut-off value K_{tol} does not play a role when Δt is smaller than ϵ^2 while the computational results have marginal difference when Δt is greater than ϵ^2. The accuracy results numerically demonstrate the proposed schemes provide the expected order of convergence in time.

5 Conclusions

We proposed and studied the higher order operator splitting Fourier spectral methods for solving the AC equation. The methods decompose the AC equation into the subequations with the heat and the free-energy evolution terms. Unlike the first and the second order methods, each of the heat and the free-energy evolution operators has at least one backward evaluation in the higher order methods. For the third order method, we suggested the three values $\omega_X, \omega_Y, \omega_Z$ at which $\max\{|a_j|, |b_j|\}$ have local minimums and we then obtained smaller error than other ω values. For the fourth order method, we used two symmetric combinations of the second order operators. And a simple cut-off function could limit exponential amplification of the high frequency modes in the heat operator and it worked well with the proposed schemes. We numerically demonstrated, using the traveling wave solution and the spinodal decomposition problem with random initial values, that the proposed methods have the third and the fourth order convergence as expected.

Acknowledgment

This research was supported by Basic Science Research Program through the National Research Foundation of Korea(NRF) funded by the Ministry of Education(2009-0093827, 2012-002298).

References

[1] S.M. Allen, J.W. Cahn, A microscopic theory for antiphase boundary motion and its application to antiphase domain coarsening, Acta Metall. 27 (1979) 1085–1095.

[2] M. Beneš, V. Chalupecký, K. Mikula, Geometrical image segmentation by the Allen–Cahn equation, Appl. Numer. Math. 51 (2004) 187–205.

[3] J.A. Dobrosotskaya, A.L. Bertozzi, A wavelet-Laplace variational technique for image deconvolution and inpainting, IEEE Trans. Image Process. 17 (2008) 657–663.

[4] L.C. Evans, H.M. Soner, P.E. Souganidis, Phase transitions and generalized motion by mean curvature, Commun. Pur. Appl. Math. 45 (1992) 1097–1123.

[5] M. Katsoulakis, G.T. Kossioris, F. Reitich, Generalized motion by mean curvature with Neumann conditions and the Allen–Cahn model for phase transitions, J. Geom. Anal. 5 (1995) 255–279.

[6] X. Feng, A. Prohl, Numerical analysis of the Allen–Cahn equation and approximation for mean curvature flows, Numer. Math. 94 (2003) 33–65.

[7] X. Yang, J.J. Feng, C. Liu, J. Shen, Numerical simulations of jet pinching-off and drop formation using an energetic variational phase-field method, J. Comput. Phys. 218 (2006) 417–428.

[8] R. Kobayashi, Modeling and numerical simulations of dendritic crystal growth, Phys. D 63 (1993) 410–423.

[9] A. Karma, W.-J. Rappel, Quantitative phase-field modeling of dendritic growth in two and three dimensions, Phys. Rev. E 57 (1998) 4323–4349.

[10] W.J. Boettinger, J.A. Warren, C. Beckermann, A. Karma, Phase-field simulation of solidification, Annu. Rev. Mater. Res. 32 (2002) 163–194.

[11] D.J. Eyre, An unconditionally stable one-step scheme for gradient systems, http://www.math.utah.edu/∼eyre/research/methods/stable.ps.

[12] X. Yang, Error analysis of stabilized semi-implicit method of Allen–Cahn equation, Discrete Cont. Dyn. B 11 (2009) 1057–1070.

[13] J. Shen, X. Yang, Numerical approximations of Allen–Cahn and Cahn–Hilliard equations, Discrete Cont. Dyn. A 28 (2010) 1669–1691.

[14] Y. Li, H.G. Lee, D. Jeong, J. Kim, An unconditionally stable hybrid numerical method for solving the Allen–Cahn equation, Comput. Math. Appl. 60 (2010) 1591–1606.

[15] H.G. Lee, J.-Y. Lee, A semi-analytical Fourier spectral method for the Allen–Cahn equation, Comput. Math. Appl. 68 (2014) 174–184.

[16] G. Strang, On the construction and comparison of difference schemes, SIAM J. Numer. Anal. 5 (1968) 506–517.

[17] D. Goldman, T.J. Kaper, Nth-order operator splitting schemes and nonreversible systems, SIAM J. Numer. Anal. 33 (1996) 349–367.

[18] S. Blanes, F. Casas, On the necessity of negative coefficients for operator splitting schemes of order higher than two, Appl. Numer. Math. 54 (2005) 23–37.

[19] H.G. Lee, J.-Y. Lee, A second order operator splitting method for Allen–Cahn type equations with nonlinear source terms, Submitted.

[20] H.G. Lee, J. Shin, J.-Y. Lee, First and second order operator splitting methods for the phase field crystal equation, Submitted.

[21] G.M. Muslu, H.A. Erbay, Higher-order split-step Fourier schemes for the generalized nonlinear Schrödinger equation, Math. Comput. Simul. 67 (2005) 581–595.

[22] R. McLachlan, Symplectic integration of Hamiltonian wave equations, Numer. Math. 66 (1994) 465–492.

[23] N. Ahmed, T. Natarajan, K.R. Rao, Discrete cosine transform, IEEE Trans. Comput. C-23 (1974) 90–93.

[24] P.C. Fife, Models for phase separation and their mathematics, Electron. J. Diff. Equ. 2000 (2000) 1–26.